Published in final edited form as:
Nutr Neurosci. 2011 July ; 14(4): 165–178. doi:10.1179/147683011X13009738172396.

Prenatal protein malnutrition alters the proportion but not numbers of parvalbumin-immunoreactive interneurons in the hippocampus of the adult Sprague-Dawley rat

James P Lister[1], **Gene J Blatt**[1], **Thomas L Kemper**[1], **John Tonkiss**[1], **William A DeBassio**[2], **Janina R Galler**[3], and **Douglas L Rosene**[1]

[1]Department of Anatomy and Neurobiology, Boston University School of Medicine, Boston, MA, USA

[2]Departments of Pediatrics and Neurology, Boston University School of Medicine, Boston, MA, USA

[3]Judge Baker Children's Center, Harvard Medical School, Boston, MA, USA

Abstract

Prenatal protein malnutrition alters the structure and function of the adult rat hippocampal formation. The current study examines the effect of prenatal protein malnutrition on numbers of parvalbumin-immunoreactive (PV-IR) GABAergic interneurons, which are important for perisomatic inhibition of hippocampal pyramidal neurons. Brain sections from prenatally protein malnourished and normally nourished rats were stained for parvalbumin and PV-IR neurons were quantified using stereology in the dentate gyrus, CA3/2 and CA1 subfields, and the subiculum for both cerebral hemispheres. Results demonstrated that prenatal malnutrition did not affect the number of PV-IR interneurons in the hippocampus. Since prenatal protein malnutrition reduces total neuron numbers in the CA1 subfield (1), this results in an altered ratio of PV-IR interneurons to total neuronal numbers (from 1:22.9 in controls to 1:20.5 in malnourished rats). Additionally, there was no hemispheric asymmetry of either PV-IR neuron numbers or ratio of PV-IR:total neuron numbers.

Keywords

Undernutrition; Hemispheric asymmetry; Inhibition; CA1 subfield; CA3 subfield; Stereology

Introduction

Prenatal protein malnutrition has been shown to affect the structure and function of the adult rat hippocampus despite postnatal dietary rehabilitation.[1–4] Electrophysiological studies have demonstrated that malnutrition impairs the establishment and maintenance of long-term potentiation, a mechanism that is believed to underlie learning and memory processes

Correspondence to: Douglas L Rosene, Department of Anatomy and Neurobiology, Boston University School of Medicine, 715 Albany Street W701, Boston, MA 02118, USA. drosene@bu.edu.

in the hippocampus.[5–7] In agreement with this, behavioral studies indicate that some aspects of learning and memory may be altered in the prenatally malnourished rat.[8] More recent work with benzodiazepines reveals involvement of the GABAergic system; prenatally protein malnourished rats are less sensitive to the amnestic effects of moderate doses of chlordiazepoxide, a non-selective benzodiazepine agonist, whether applied systemically[9] or applied directly to the medial septum.[10] Additionally, electrophysiological studies using a kindling model of seizure activity also show that prenatally malnourished rats spend greater periods of time at each stage of kindling and do not reliably reach the final stage of kindling characterized by generalized motor convulsions;[11] this alteration of the normal pattern of kindling is consistent with greater inhibition of the principal cell population. Following kindling, an early study of paired-pulse measures showed that granule cells in the prenatally malnourished rat are more inhibited in response to the second pulse compared to control animals,[12] but this inhibition was later found to be dependent on factors such as the amplitude of the first population spike, the duration of interval to the second pulse, the behavioral state of the animal, and the age of the animal.[13,14] The most direct evidence for increased inhibition in the prenatally malnourished hippocampus comes from studies that showed a greater frequency of miniature inhibitory postsynaptic potentials (IPSPs) in both CA1 pyramidal neurons[15] and CA3 bipolar interneurons[16] of prenatally malnourished rats compared to controls. This suggests either increased number of inhibitory synapses or increased probability of quantal release per synapse.

Thus one possible mechanism for the elevated frequency of miniature IPSPs could be a greater number of presynaptic contacts from inhibitory interneurons on each postsynaptic target.[15] Previous studies have reported only modest effects of malnutrition on hippocampal morphology, such as decreases in dendritic spine density and soma size,[17–19] but no study has directly quantified inhibitory synapse numbers in the prenatally malnourished hippocampus. However, as previously reported,[1] prenatal protein malnutrition does reduce neuron number in the principal cell layer of the CA1 subfield in adult rats while leaving the rest of the hippocampus unchanged. Prenatally malnourished rats were found to have 12% fewer total neurons in CA1, but since this was a measurement of total number of neurons, it is unknown whether the insult affected equally both principal neurons and interneurons. This is important since if inhibitory interneurons are spared and principal neurons reduced by prenatal malnutrition, enhanced inhibition might result from an altered ratio of inhibitory to excitatory neurons in CA1.

One strategy for assessing the effects of prenatal protein malnutrition on the GABAergic system would be to quantify the total number of inhibitory GABAergic interneurons. However, the rat hippocampus contains a diverse array of inhibitory interneurons with different structural and functional characteristics.[20,21] Quantifying the entire inhibitory population might obscure any differential effects on individual interneuron subpopulations, and a decrease in one subpopulation might not be noticed if there was a compensatory increase in another subpopulation. An alternate strategy is to utilize population-specific markers to quantify separate varieties of interneurons. While more time consuming and labor intensive, this approach can reveal subpopulation-specific effects on the GABAergic system.

Recently, studies using both perinatal[7] and prenatal[22] nutritional insults have indicated effects on select hippocampal interneuron populations (neuronal nitric oxide synthase-positive (nNOS+) and glutamic acid decarboxylase 67-positive (GAD67+) interneurons, respectively). The current study adds to these findings byexamining the effect of prenatal protein malnutrition on another distinct subpopulation of interneurons, the parvalbumin-immunoreactive (PV-IR) neurons in the adult rat hippocampus. Parvalbumin-immunoreactive (PV-IR) neurons were selected for quantification for two reasons. First, interneurons that express parvalbumin are predominantly chandelier cells and basket cells (~75–85%, from Baude *et al.*[23]) that provide inhibition to pyramidal neurons at the axon initial segment and cell body, respectively.[20] These cells are thus an important population for regulating output from the pyramidal cells and a change in this population would affect synaptic transmission through the hippocampus. PV-IR neurons in the hippocampus also include 'oriens lacunosum-moleculare' cells (O-LM cells) and bistratified cells, GABAergic interneurons whose axons target the dendrites of pyramidal neurons in the CA1 subfield and thus also play a role in inhibiting the principal cell populations. Bistratified cells specifically target the dendrites of CA1 pyramidal neurons in the stratum radiatum and stratum oriens, whereas O-LM cells restrict their axon terminations to the CA1 pyramidal dendrites in the stratum lacunosum-moleculare.[20,21] Second, PV-IR neurons comprise approximately half the population of interneurons in the stratum pyramidale of CA1 where prenatally malnourished rats had a reduced total number of neurons as previously reported.[1] This study quantifies the distribution of PV-IR interneurons in the major subfields of the hippocampus of prenatally malnourished compared to control rats to determine whether there are any changes in the population of these interneurons that could account for altered inhibition.

Materials and methods

Subjects and animal procedures

The subjects of this investigation are the same subjects used for studies of hippocampal total neuron numbers[24] and total neuron number asymmetries.[1] Briefly, Sprague-Dawley rats (VAF plus, Charles River Laboratories, Kingston, MA, USA) were maintained in the Laboratory Animal Science Center of Boston University Medical Center which is fully accredited by the Association for the Assessment and Accreditation of Laboratory Animal Care. All experiments were conducted in strict accordance with the guidelines of the NIH *Guide for the care and use of laboratory animals* and the *U.S. Public Health Service Policy on humane care and use of laboratory animals* and were approved by the Institutional Animal Care and Use Committee at Boston University Medical Campus.

Nutritional treatment

Nulliparous female rats were allowed *ad libitum* access to one of two isocaloric diets (Teklad, Madison WI, USA) that differed in casein protein content. One diet contained adequate protein (25% casein) whereas the second diet had a low level of protein (6% casein). Female rats were introduced to these diets 5 weeks prior to mating in order to allow for metabolic adjustment to the diet. Male rats were likewise acclimated to the same diets but for 1 week just prior to mating. Litters from both prenatally malnourished and normally nourished dams were culled to eight pups each (six males and two females) and whole litters

from all dams were fostered to well-nourished mothers who had given birth no more than 24 hours previously. Pups exposed to the 6% casein diet during gestation and cross-fostered to lactating dams given the 25% casein diet are designated ‘6/25’. Pups exposed to the 25% diet during gestation and cross-fostered to lactating dams given the 25% casein diet are designated ‘25/25’. Rats were weaned onto regular laboratory chow (Purina, formula 5001) at postnatal day 21 and subsequently housed in same-gender littermate group of 2 or 3.

Tissue processing

One 90-day old male rat was chosen randomly from each of 10 litters of 25/25 animals and 10 litters of 6/25 animals and subsequently blind-coded into two separate cohorts. Subjects were deeply anesthetized with an intraperitoneal injection of sodium pentobarbital and transcardially perfused with 4% paraformaldehyde in 0.1 M phosphate-buffer solution (PBS) (pH 7.4) for 5 minutes (approximately 250 ml of fixative). Brains were immediately removed and cryoprotected in a series of glycerol solutions (24-hour incubation in 10% glycerol with 2% dimethylsulfide (DMSO) in 0.1 M PBS, pH 7.6, followed by a 24-hour incubation in 20% glycerol with 2% DMSO in 0.1 M PBS, pH 7.6) and then flash-frozen in 2-methylbutane at −75°C as previously described.[25] Brains were stored at −80°C until sectioned horizontally on a freezing microtome at a thickness of 30 μm and collected in eight interrupted series, resulting in a section spacing of 240 μm. Sections reserved for immunohistochemistry were collected in 15% glycerol in 0.1 M PBS (pH 7.6) and returned to −80°C until stained for parvalbumin.

The first section to be saved in every brain was randomly selected prior to reaching the level of the hippocampus, which ensures that each series has a random starting location within the hippocampus. This process yields series of systematically random sections which is a prerequisite for using the optical fractionator method.[26] One series per brain was selected from the stored series for immunohistochemical staining for parvalbumin. This series was removed from the freezer and allowed to come to room temperature. Sections from all subjects were ‘batch-processed’ simultaneously in the same solutions to ensure consistent staining between cases.

The protocol for staining was as follows. For immunohistochemistry, sections were removed from the freezer, allowed to thaw to room temperature, and then rinsed in three 8-minute baths of 0.1 M Tris-buffered saline (TBS) (pH 7.6) to remove the glycerol solution. They were then transferred for 33 minutes to a 1% H_2O_2 solution to quench endogenous peroxidase activity. Sections were then rinsed in 0.1 M TBS three more times, 8 minutes per bath. In order both to block non-specific binding and to gently open the cell membranes for improved penetration of the antibodies, sections were incubated for 90 minutes in a solution composed of 0.1 M TBS containing 0.25% bovine serum albumin and 0.1% Triton-X (Tris-BSA-Tx at pH 7.6). Sections then were incubated for 36.5 hours on a rocker at 4°C in the primary antibody (monoclonal mouse immunoglobulin G (IgG), which binds specifically to the calcium-binding domain of parvalbumin, catalog #235, Swant, diluted 1:5000 in Tris-BSA-Tx).

Following primary antibody incubation, tissue sections were rinsed three times in Tris-BSA-Tx for 10 minutes per bath and then incubated for 2.25 hours in a secondary antibody

(biotinylated anti-mouse IgG, Vector Labs, Burlingame, CA, USA). After this incubation tissue sections were rinsed three times in Tris-BSA-Tx for 10 minutes each and then incubated for 85 minutes with the ABC elite solution (Vectastain Elite ABC kit (Standard), Vector Labs, Burlingame, CA, USA), which forms a complex of avidin–biotinylated peroxidase. The avidin–biotinylated peroxidase complex binds with the biotin conjugated to the secondary antibody via empty binding sites on the avidin protein. Sections were rinsed three times (5 minutes/rinse) with 0.1 M TBS and then stained in a diaminobenzidine (DAB) solution (50 mg DAB, 40 mg ammonium chloride, 0.3 mg glucose oxidase, and 200 mg beta-D-glucose dissolved in 100 ml of 0.1 M TBS) for 25 minutes. Many immunohistochemical protocols add hydrogen peroxide directly to the staining solution. In this protocol hydrogen peroxide is generated by the glucose oxidase reacting with glucose. This limits the reaction of DAB with the peroxidase to the rate at which hydrogen peroxide is produced by the glucose oxidase reaction.[27–29] The DAB chromogen is oxidized by free oxygen generated by the peroxidase to form an insoluble dark reaction product. The 25-minute reaction time period was determined in trial series to be optimal for adequate staining of immunoreactive neurons with low background staining and was identical for all cases. Greater control over the rate of tissue staining is thus achieved and the optimal staining time can be controlled with increased precision. Sections were washed three more times for 5 minutes per wash in 0.1 M TBS to clear the tissue of the DAB chromogen and quench the staining reaction. Sections were then mounted on gelatin-subbed slides and allowed to air dry, then dehydrated in ethanol, cleared with xylene, and coverslipped with Permount (Fisher Scientific, Waltham, MA, USA).

Negative controls included tissue sections that were processed identically and in parallel with experimental sections as described above except that control sections were incubated without either the primary antibody, the secondary antibody, or the avidin–biotin solution. All negative control sections exhibited no specific or non-specific staining. The distribution of parvalbumin immunoreactivity has been surveyed extensively in many regions of the rat brain, including the hippocampus. The staining patterns produced in the tissue from both prenatally malnourished and normally nourished subjects conform identically to that previously described,[27–29] as can be seen by comparing the photomicrographs in Fig. 1 to photomicrographs from earlier studies.

Definition of anatomical areas

Exhaustive descriptions of hippocampal cytoarchitecture, including the dentate gyrus, the CA3/2 and CA1 subfields, and the subiculum, are available in several published accounts.[30,31] These regions were outlined identically to the regions assessed for total number of neurons in a Nissl-stained series of sections as reported previously.[1] Thus PV-IR cell bodies were quantified in the same layers for which total neuronal number was estimated which included the hilus of the dentate gyrus, the strata pyramidale of CA3/2 and CA1, and the cellular layers of the subiculum. In addition, the granule cell layer of the dentate gyrus and strata oriens of CA3/2 and CA1 were included in this analysis of PV-IR neurons. The granule cell layer was included because PV-IR cells are sufficiently dispersed to be easily identified, in contrast to the Nissl stained material where the dense packing of granule cells makes counting very difficult. The strata oriens in CA3/2 and CA1 were

included because the PV-IR interneuron population is distributed across both stratum pyramidale and oriens with a substantial number of cells just subjacent to the pyramidal cell layer. Exclusion of the stratum oriens would ignore a significant component of the functional inhibitory input to the initial axon segment and soma of the pyramidal cells. In contrast, there are nearly no PV-IR interneurons present in the strata moleculare and radiatum of the hippocampus so these layers were not included in the analysis.

The regional borders used for stereological quantification are illustrated in Fig. 2 which show a transverse section of the hippocampal formation stained for parvalbumin. The stained terminals of the PV-IR interneurons form characteristic baskets around the unstained pyramidal cells and this staining pattern reveals the cytoarchitectonic features of the hippocampus, allowing individual subfields to be discerned at low power with the same accuracy as with Nissl stains. The granule cell layer of the dentate gyrus is easily determined by the honeycombed appearance of stained terminals outlining the small, densely packed granule cells. Interposed between the two blades of the granule cell layer lies the hilus of the dentate gyrus, except where the densely packed pyramidal neurons of the proximal CA3 layer extend into the hilus. The border of the hilus has been modified to ensure that the same area is measured as in the previous study.[1] The border is extended from the tips of the granule cell layer perpendicular to the stratum pyramidale of CA3. Small portions of stratum oriens and radiatum of CA3 are therefore included. Due to the relatively small size of the CA2 subfield and the difficulty of reliably establishing its border with CA3, it was grouped with the CA3 subfield and quantified as one area designated as CA3/2. The pyramidal layer of the CA3/2 subfield can be determined by the large honeycombed ‘empty baskets’ formed by the PV-IR terminals around the unstained pyramidal cell bodies. Deep to the stratum pyramidale is the stratum oriens of CA3/2 which is defined by the lack of the aforementioned closely packed ‘honeycombs’ and obliquely oriented PV-stained fibers. Stratum oriens is distinguished from the alveus by a sharp transition from uniform background staining to the striated appearance caused by the ordered layering of axons in the alveus; the alveus also contains very few PV-IR fibers. The border of CA3/2 with CA1 was identified where the large ‘empty baskets’ of the CA3/2 neurons give way to smaller, more densely packed ‘empty baskets’. This change corresponds to the shift in morphology from the larger pyramidal cells of CA3/2 to the more densely packed and smaller pyramidal neurons of CA1. The stratum oriens of CA1 is similar in appearance to the same layer in CA3. The proximal border with stratum oriens of CA3 is drawn as an extension of the border between the stratum pyramidale of these subfields down to the alveus. The distal border with the subiculum is defined where the relatively sparsely populated stratum oriens narrows and is replaced by the more frequent baskets of the subicular pyramids. The prosubicular transition zone at the distal end of the CA1 subfield was included with the stratum pyramidale of CA1 due to its small size and the difficulty of reliably separating it from CA1. The border between the prosubiculum and the subiculum, however, was more reliable and corresponded to where the stratum oriens of CA1 ends and the large, less densely packed ‘empty baskets’ of the subicular pyramidal cells begin to replace the dense and closely packed ‘empty baskets’ of CA1 and prosubicular neurons. The distal border of the subiculum was identified where the ‘empty baskets’ marking the loosely organized, large subicular neurons give way to ‘empty baskets’ characteristic of the smaller neurons of the

presubiculum. Outlines of these areas were periodically checked against outlines drawn on Nissl-stained sections of nearby series from the same subject to verify consistency and ensure that the correct regional boundaries were used.

Stereology

Quantification of PV-IR neurons was performed using the Bioquant Nova V5.50.8 program (Bioquant Image Analysis Corporation, Nashville, TN, USA) on a computer connected to a Nikon E600 microscope with a motorized stage and an Optronics video camera. The optical fractionator technique, a method of design-based stereology, was used to obtain estimates of total PV-IR neuron numbers within each area.[26,32] A systematically random series of sections spaced equi-distantly through the entire extent of the hippocampus was used for quantification. Brains were selected for analysis in a random order, and a Gellerman schedule[33] was used to alternate hemispheres randomly so that no more than two left or two right hemispheres were analyzed in a row. Only one hemisphere from each brain was randomly selected and quantified in a first round, and then the remaining hemispheres were quantified in a second round so that the left and right hippocampal formations from the same brain were quantified separately several months apart. Slides were coded during quantification to ensure that the investigator was blind to group membership.

During quantification, the regions of interest for all subfields were outlined at 4× magnification with the Bioquant software. Neuron counts were conducted using a high numerical aperture 60× oil immersion lens. Stained neurons were identified by the presence of dark brown to black colored reaction product filling the cell body. The neuronal cell body was used as the counting object. Neuron cell bodies were identified morphologically by a soma of at least 8 μm in diameter and the presence of darkly stained processes extending from the soma. Examples of a stained neuron that would be counted and an ambiguous object that would not be counted are presented in Figs 3A and B.

The systematic random sampling of sections is represented during estimation in the optical fractionator technique by the section sampling fraction (SSF), which is the number of sections sampled divided by the total number of sections containing the region under study.[34] In order to reduce error associated with between section variability, the appropriate SSF for each region was determined by pilot studies. The granule cell layer and the hilus of the dentate gyrus, as well as the stratum oriens of CA3, were measured with a SSF of 1/8. The stratum pyramidale layers of CA1 and CA3 were measured with an SSF of 1/16. The stratum oriens of CA1 and the subiculum were measured with an SSF of 1/24. These SSF values yielded a minimum number of seven sections for each region that was sampled.

Sampling grids of known dimensions were positioned over each outlined region of interest. A pilot study determined the appropriate dimensions for each grid in order to maximize the sampling efficiency of the study. For the hilus and granule cell layer of the dentate gyrus, the stratum pyramidale and the stratum oriens of CA3, and the subiculum, grid dimensions were 100 μm in both the *x* and *y* directions. For the stratum pyramidale and the stratum oriens of the CA1 subfield, a grid of 90 μm in both the *x* and *y* directions was used. In all areas but the subiculum, the disectors placed at each grid intersection measured 75 μm on each side. For the subiculum, the disector frame measured 50 μm on each side.

The thickness sampling fraction (TSF) is defined as the thickness of the tissue probed by the disectors divided by the actual thickness of the section. Each disector was raised through the entire thickness of the tissue at each grid intersection, and therefore the TSF for all regions equals 1. PV-IR neurons were counted within the disectors provided they were not located at the bottom cut surface, designated the exclusion plane, and did not encounter either of the two 'forbidden' lines of the disector frame. Guard volumes above and below the disector were not implemented in order to maintain consistency with the methods used to collect data on total neuronal numbers;[1] this ensures greater comparability of the present findings to that data. This lack of guard volumes and the implications for the current data are addressed in the Discussion under Technical considerations. The counts produced by sampling known fractions of the tissue with disectors comprise a systematic random sampling of the entire hippocampus and are used to generate an estimate of the true number of neurons within each region; when averaged together, the estimates from individual subjects will converge on the true population value.[26]

Data analysis

Neuronal number data were analyzed using a three-way analysis of variance (ANOVA) with nutrition as a between-subjects factor and hemisphere and region as within-subject factors. The significant main effect of region was followed-up with Bonferroni *post hoc* analyses to identify the source of the significance.

Ratios of PV-IR interneurons to total neuronal number for the CA3/2, CA1, and subiculum were analyzed using a three-way ANOVAwith nutrition as a between-subjects factor and hemisphere and region as within-subjects factors. The ratio data for the CA subfields are calculated using the combined estimates of PV-IR neurons in stratum pyramidale and stratum oriens, as these cells all provide inhibition to the pyramidal neurons and are thus a more relevant functional measure.

Results

To determine whether prenatal protein malnutrition affected the numbers of PV-IR interneurons in the hippocampus, neuron numbers were estimated for seven regions of the hippocampal formation: the hilus of the dentate gyrus, the granule cell layer of the dentate gyrus, the stratum pyramidale of the CA3/2 subfield, the stratum oriens of the CA3/2 subfield, the stratum pyramidale of the CA1 subfield, the stratum oriens of the CA1 subfield, and the principal cell layer of the subiculum. These regions were quantified separately in both left and right hemispheres of prenatally malnourished and control rats in order to detect any hemispheric differences in neuron numbers. Table 1 presents the means of these data along with the coefficients of error (CEs).[32] Figs 3A and B are photomicrographs taken at high magnification showing representative examples of PV-IR neurons in the hippocampus.

Effect of region

A three-way ANOVAwas performed to investigate any group differences in the data. This analysis found a significant main effect for region ($P < 0.0001$) which was not surprising since the estimates for total PV-IR neuronal number vary substantially from region to

region. Bonferroni *post hoc* tests investigating the main effect of region revealed significant differences between the means for nearly all regions (collapsed across nutritional group and hemisphere). As shown in Fig. 4, the only comparisons that were not significant were the comparisons between the hilus and the granule cell layer, the hilus and stratum oriens of CA3, and the granule cell layer and stratum oriens of CA3. The mean numbers of PV-IR neurons contained within the hilus, the granule cell layer of the dentate gyrus, and the stratum oriens of CA3 were similar. The remaining regions all were significantly different in the mean number of PV-IR interneurons.

Effect of hemisphere

The three-way ANOVA also showed there was no effect of hemisphere ($P > 0.4$) and no hemisphere by nutrition interaction ($P > 0.3$) or hemisphere by region interaction ($P > 0.5$). Fig. 5 shows the mean number of PV-IR interneurons for the different regions in both hemispheres collapsed across nutritional group due to the absence of any significant effects of the nutrition factor or significant interactions with the nutrition factor.

Effect of nutrition

The three-way ANOVA demonstrated that there was no significant main effect of nutrition ($P > 0.5$) indicating that malnutrition did not affect the total number of PV-IR interneurons across all the subfields. Additionally, there were no significant nutrition by region ($P > 0.9$) or nutrition by hemisphere ($P > 0.3$) interactions. The mean number of PV-IR interneurons for the two nutritional groups are presented in Fig. 6; the data are collapsed across hemisphere due to the absence of any significant effects of the hemisphere factor or significant interactions with the hemisphere factor.

Effect of nutrition on the ratio of PV-IR interneurons to total neurons

While there was no evidence that the prenatal malnutrition altered the number of PV-IR neurons, our previous report[1] that there was a nutrition-induced reduction in the number of neurons in CA1 led us to investigate the ratios of PV-IR interneurons to total number of neurons in the CA3/2, CA1, and subiculum subfields. This was done using the estimates of PV-IR neuron number reported here and the values for total neuron number from the same subjects reported previously.[1] No such ratio was determined for the dentate gyrus since there was no available data on the number of granule cells. During calculation of ratios for each subfield, the value used for PV-IR neurons is the combined number of PV-IR interneurons counted in the pyramidal and oriens layers. This combined value was used since PV-IR interneurons in both layers are responsible for perisomatic inhibition of the adjacent pyramidal neurons.[20] The ratio data were analyzed using three-way ANOVA.

The three-way ANOVA showed a significant main effect of nutrition ($P < 0.03$) on the ratios of PV-IR interneurons to total neuron number (Fig. 7). The well-nourished rats have a ratio of 0.044 (one PV-IR interneuron for every ~22.9 total neurons), whereas the prenatally malnourished rats have a ratio of 0.049 (or one PV-IR interneuron for every ~20.5 total neurons). This suggests there may be fewer total neurons for every PV-IR interneuron in the prenatally malnourished rats compared to the well-nourished controls. There were no significant nutrition by hemisphere interactions or significant main effect of hemisphere.

There was a significant main effect of region ($P < 0.0001$) which is expected due to the variability in both PV-IR interneurons (as noted above) and in total numbers of neurons[1] from region to region.

Discussion

Technical considerations

As previously described,[24] the stereological method used in this experiment differs from the normal implementation of the optical fractionator[26] only in that guard volumes were not used. The omission of guard volumes from the quantification protocol for the Nissl-stained tissue was motivated by the extensive shrinkage of the frozen sections in the *z*-dimension from 30 μm at the time of cutting to approximately 6–7 μm after processing.[24] Using a high numerical aperture oil immersion lens and a motorized stage capable of fine movements in the *z*-axis, we were able to focus through the section, exclude those cells in focus at the bottom of the section and then observe and count cells that came into focus as the focal plane was raised through the section. Thus satisfies the unbiased counting rules required by the optical fractionator method – excluding objects sampled by three exclusion planes, counting only the leading edge of the counting object as it came into focus.

However, such extensive shrinkage severely reduced the ability to implement guard volumes of any meaningful size without severely reducing the volume of tissue available for quantification (see[1,24] for a more detailed discussion). Guard volumes protect against the introduction of bias in stereological estimates by reducing the contribution of edge effects such as lost caps that result when staining of objects located at the cut surfaces of sections is diminished in size or lost due to damage caused by the microtome blade.[35] Guard volumes placed above and below the disector are regions of tissue in which counting is not performed in order to control errors resulting from these edge effects.[36]

Implementing guard volumes of, for instance, 2 μm at the top and bottom of the tissue in this study would have yielded only 2–3 μm of tissue for probing with the optical disector; despite the resolution of our microscopy equipment, at that thickness the effective result is very nearly a two-dimensional plane and an exclusion plane in the *z*-axis would be impossible, since virtually every object in the tissue would intersect this plane and thus be excluded. We could not implement a physical disector method since adjacent sections were not always available for staining. Since two-dimensional profile counts rely on assumptions regarding the mean diameter of the counting objects, and changes in cell size have been reported in this model of protein undernutrition[18,19] that would confound results from an assumption-based profile counting method, retaining the optical fractionator method without guard volumes was the best remaining option.

The effect of not using guard volumes is consistently an underestimate of the true total number of neurons according to unpublished work (Bowley *et al.*, in preparation) which examined differences in glial number estimated in the white matter of rhesus macaques by counting the same areas first with and then without guard volumes. The results of that work indicate that not using guard volumes results in an underestimate of about 10% relative to the estimates obtained with guard volumes. Using guard volumes would have produced

unbiased estimates of the total number of PV-IR interneurons in the measured hippocampal subfields and facilitated comparisons to other reports in the literature; however, the goal of the present study was to investigate this neuronal population in the malnourished rat and relate the results to previous findings. Thus for that reason, and the reasons detailed above, a counting protocol identical to that used in previous studies was used. In the current experiment, the staining of all tissues occurred simultaneously in the same solutions, and thus this procedural underestimate should apply equally to all groups and therefore would not affect comparisons between the different hemispheres or nutritional groups.

It should also be noted that for purposes of consistency, the border of the hilus of the dentate gyrus was modified as in the Nissl studies[1,24] to include small portions of the strata oriens and radiatum of the CA3 subfield that extend into the hilus. Therefore the values of PV-IR interneurons in the hilus are slight overestimates, and the values in the CA3 stratum oriens are slight underestimates of the true values.

PV-IR interneurons in the hippocampal formation

The majority (~75–85%) of PV-IR interneurons in the hippocampal formation are basket and chandelier cells.[20,23,37] These neurons distribute their axons within the principal cell layers and form inhibitory synapses on the cell bodies and axon initial segments of pyramidal neurons.[38–41] These interneurons are therefore positioned to control output from the principal cells of the hippocampus, and individual interneurons can reach targets in the thousands. For instance, it was estimated that a single chandelier cell innervates ~1200 pyramidal cells in the CA1 subfield.[42] The remaining 15–25% minority of PV-IR interneurons are O-LM and bistratified neurons in the CA subfields that provide inhibition at the pyramidal neuron dendritic arbor.[21,23] O-LM cells have their somata in the stratum oriens, receive recurrent collateral input, and provide inihibition to apical dendrites in the stratum lacunosum-moleculare, where pyramidal neurons receive entorhinal input. Bistratified neurons have their cell body in or near to the stratum pyramidale, receive recurrent collateral input and input from the upstream subfield (mossy fiber input to CA3; Schaffer collateral input to CA1), and their axonal terminations are confined to stratum radiatum and stratum oriens thus coinciding with upstream inputs and recurrent collaterals. These cell populations appear somewhat complementary O-LM cells are positioned to provide input to dendrites at the location of extrinsic (entorhinal inputs) while bistratified cells are positioned to provide input to dendrites at the location of intrinsic hippocampal inputs (mossy fiber input from granule cells, Schaffer collateral input from CA3 cells, and recurrent collaterals). These differences in input-output relationships, as well as differences in spike timing and other electrophysiological properties, suggest a ‘division of labor’ among different inhibitory subpopulations.[21]

The tissue stained for parvalbumin in this study did not differ from the morphological findings described above. Immunoreactive cell bodies were localized to the pyramidal cell layers, the hilus of the dentate gyrus, and the strata oriens of CA3/2 and CA1. Labeled axon terminals were found almost exclusively in the principal cell layers, forming baskets that mark the locations of unstained pyramidal neurons. Therefore, the neurons quantified in this study encompass a large subpopulation responsible for controlling output from the

pyramidal neurons (chandelier and basket cells),[20] as well as a small proportion of interneurons targeting dendrites.

Numbers of PV-IR neurons

In the present study we used stereological methods to obtain an estimate of about 10 300 PV-IR neurons in the CA1 subfield of control animals and 6500 in the CA3 subfield. The majority of studies of PV-IR neuron numbers in the rat hippocampal formation to date have measured numerical density as opposed to estimating total neuron number.[43–45] This complicates direct comparisons to the current findings, especially since many of these studies do not also measure volumes that could be used to estimate the total number from the density of cells. As an example, one study that measured numerical density of PV-IR neurons in subdivisions of the hippocampus reported 4900 and 8300 cells per mm^3 for the CA3 and CA1 strata pyramidale, respectively.[45] Those numerical densities project total numbers of approximately 14 000 and 18 600 PV-IR neurons in CA3 and CA1, respectively, using the volumes observed in our study of total neuron numbers.[1] These values are thus substantially higher than the estimates of PV-IR interneuron number produced in the current study. However since Nomura and colleagues did not measure the total volume of the measured layers, it is unknown how differences in volume measurements may have contributed to the discrepancy in findings.

Studies using methods of unbiased stereology similar to the method used here have reported estimates of PV-IR neurons that are closer to the current values than studies of numerical density would suggest. One study of neuronal numbers in the hilus estimate the number of PV-IR neurons to be 2944.[46] While this value is still higher than estimate reported here of 1744 neurons, the difference between estimates is substantially less in magnitude than the differences found when comparing to the reports of numerical densities. Another study that used stereology to quantify the number of PV-IR neurons in strata pyramidale and oriens of CA1 estimated 2772 and 2656 cells contained in those layers, respectively,[47] for a total of 5428. While lower than the estimates reported here for those layers, the differences are much closer than those based on numerical density. It is important to reiterate that due to the lack of guard volumes, our estimates will be slightly biased underestimates of the total number, and this will contribute to differences when compared to other data in the literature.

In addition to variation that may be due to methodology, differences in rat strain used in these studies may also contribute to the variation found in estimates. The estimates reported here were derived from measurements made in Sprague-Dawley rats whereas the other studies mentioned, with the exception of the report by Buckmaster and Dudek, used either Long-Evans or Wistar rats. It should be noted that the estimate for PV-IR neurons in the hilus from the Buckmaster study, which used the Sprague-Dawley strain of rat, was closest in value to the estimate reported here.

Numbers of PV-IR interneurons are symmetrical between hemispheres

Asymmetries in morphological measures of the rat hippocampus, including neuronal number and density of neurons, have been reported.[1,48–51] Our previous study showed the right hemisphere has 6 and 21% fewer total neurons in the CA3 and CA1 subfields, respectively,

than the left hemisphere.[1] The results of the current study demonstrate however that corresponding asymmetries are not found in the numbers of PV-IR interneurons.

The causes of asymmetries in the rat hippocampus are unknown, but certain asymmetries may depend upon early life experiences. Tang and colleagues showed that the pattern observed in control rats of larger volume in the left hippocampus compared to the right hippocampus was reversed in the experimental subjects that were exposed to a novel environment during the first two postnatal weeks.[52] However their measures do not identify which components of the tissue (neurons vs. glia, or cell bodies vs. processes, for example) are responsible for the asymmetry. In contrast, prenatal protein malnutrition did not affect asymmetries of total neuron number, despite being an early life insult with demonstrable alterations to the rat hippocampus.[1] Malnutrition also does not affect the symmetry of the PV-IR subpopulation of interneurons.

It is not clear why total number of neurons in the CA3/2 and CA1 subfields of the rat hippocampus are asymmetrical between the two hemispheres yet PV-IR interneurons are distributed equally, but this suggests that the asymmetry is in the population of principal projection neurons and may reflect the different developmental origin of the pyramidal cells and interneurons. Interneurons generally derive from the ventral telencephalon (the medial ganglionic eminence in particular for PV-IR interneurons) whereas principal projection neurons derive from the subventricular zone of the dorsal telencephalon during development.[50] It is likely that neurons developing from these different sources may be subject to different processes regulating the number of neurons generated. For example, it could be that early network experience affects the generation or survivability of principal neurons but not interneurons like the PV-IR population. Hence lateralization of early experience might facilitate production or survival of principal neurons on one side but not affect non-pyramidal cells like the PV-IR population.

Another possible reason for the lack of asymmetry in PV-IR interneurons could be related to the role these cells play in neuronal circuitry. As described in the preceding section, PV-IR interneurons are mostly basket and chandelier cells and have an important role in controlling overall population activity of excitatory pyramidal cells.[54] The generation of PV-IR interneurons may be hardwired into the developmental plan in order to ensure a sufficient level of inhibition from the start, whereas the generation of excitatory projection neurons may be more plastic to adapt to the active needs of the developing nervous system.

Malnutrition does not affect PV-IR interneurons

Malnutrition has been shown to reduce the total number of neurons in the stratum pyramidale of the CA1 subfield by 12%, or approximately 35 000 neurons.[1] PV-IR interneurons were quantified in the same subjects that exhibited this reduction of total neuronal number. As shown in Fig. 6, no effect of malnutrition on the numbers of PV-IR interneurons was found in any region or layer of the hippocampal formation, which indicates that the reduction in total neuron numbers must be due to a deficit in neuronal populations that do not express parvalbumin. PV-IR cells constitute approximately half of the interneurons localized to the pyramidal layer, about 6600 neurons in CA1 of control animals by the current estimate. An insult confined to interneurons that do not express parvalbumin

could not account for the magnitude of cell loss observed in the prenatally malnourished animals. A deficit of 35 000 total neurons means that even if every one of the other ~6600 non-PV-IR interneurons were lost due to malnutrition, there would still be ~28 000 neurons missing that would have to be attributed to loss from the principal cell population itself.

Implications of altered ratios of PV-IR neurons to total neuron number

A long-standing hypothesis in this paradigm of prenatal protein malnutrition has been that the nutritional insult may affect GABAergic interneurons preferentially,[3] and indeed some studies have shown changes in the density or numbers of select GABAergic subtypes.[7,22] The current study provides more support for the idea that the inhibitory system plays an important role in malnutrition-related alterations of cognition and behavior, but interestingly this is not by way of alterations in the subpopulations of inhibitory cells themselves. Rather, this study demonstrates that numbers of PV-IR interneurons are actually spared by the nutritional insult; but taken in context with a decrease in overall neuron number, the current data shows a significant effect of nutrition on the ratios of PV-IR neurons to total neuron number. This finding underlines the need to consider not only the alterations induced by nutritional insults but also the preservations of structure and function, and how the two may interact to produce the overall observed dysfunctions. Preservation of PV-IR interneurons in prenatally malnourished animals despite a decrease in total neuronal number of the stratum pyramidale of the CA1 subfield is consistent with the earlier observations of increased inhibition in the hippocampus of prenatally malnourished rats and supports the hypothesis that imbalances of cell ratios is one factor underlying cognitive changes observed in this model of prenatal protein malnutrition.[3] In the control subjects, the average ratio of the number of PV-IR interneurons to the total number of neurons is 1 to 22.9. In the prenatally malnourished animals, the ratio of PV-IR interneurons to total neurons is 1 to 20.5. Thus in the prenatally malnourished rats there may be more inhibitory neurons responsible for mediating perisomatic inhibition per excitatory neuron. Luebke *et al.*[15] reported that prenatal protein malnutrition increased the frequency of miniature inhibitory postsynaptic currents in CA1 pyramidal cells and noted in their discussion that this might be due to an increase in the number of interneurons forming synapses on an individual cell. The increased ratio of PV-IR interneurons to total neurons reported here is consistent with that possibility. However further studies using other techniques (such as electron microscopy) are required to establish whether the preserved population of PV-IR interneurons in the prenatally malnourished rats forms the same number of synapses, but on a reduced number of targets, compared to the population in the control subjects.

Conclusion

The current study examined the effect of prenatal protein malnutrition on the number of parvalbumin immunoreactive interneurons in the rat hippocampus, which includes a majority of the interneurons that provide perisomatic inhibition to hippocampal pyramidal neurons. The results show that malnutrition did not have any effect on the numbers of these inhibitory cells. It also demonstrated that the PV-IR subpopulation of non-pyramidal cells does not show the hemispheric asymmetry of total neurons favoring the left CA1 subfield. In concert with a reduction of total neuron number in the CA1 subfield due to prenatal

malnutrition, the stability of PV-IR neuron number suggests that an increase of 11.9% in the ratio of PV-IR interneuron number to total neuron number may contribute to the reported increased inhibition in the prenatally malnourished hippocampus. Whether the demonstrated alteration in PV-IR ratios between nutritional groups has physiological consequences remains to be determined.

Acknowledgments

This work was supported in part by NIH grants MH074811, P01-HD022539, and P01-AG000001.

References

1. Lister JP, Tonkiss J, Blatt GJ, Kemper TL, Debassio WA, Galler JR, et al. Asymmetry of neuron numbers in the hippocampal formation of prenatally malnourished and normally nourished rats: a stereological investigation. Hippocampus. 2006; 16(11):946–58. [PubMed: 16983649]
2. Galler, JR.; Shumsky, JS.; Morgane, PJ. Malnutrition and brain development. In: Walker, W.; Watkins, J., editors. Nutrition in pediatrics. Neuilly-sur-Seine, France: B.C. Decker, Inc; 1996. p. 196-212.
3. Morgane PJ, Mokler DJ, Galler JR. Effects of prenatal protein malnutrition on the hippocampal formation. Neurosci Biobehav Rev. 2002; 26(4):471–83. [PubMed: 12204193]
4. Tonkiss J, Galler J, Morgane PJ, Bronzino JD, Austin-LaFrance RJ. Prenatal protein malnutrition and postnatal brain function. Ann N Y Acad Sci. 1993; 678:215–27. [PubMed: 8494264]
5. Austin KB, Bronzino J, Morgane PJ. Prenatal protein malnutrition affects synaptic potentiation in the dentate gyrus of rats in adulthood. Brain Res. 1986; 394(2):267–73. [PubMed: 3021287]
6. Bronzino JD, Austin-LaFrance RJ, Mokler D, Morgane PJ. Effects of prenatal protein malnutrition on hippocampal long-term potentiation in freely moving rats. Exp Neurol. 1997; 148(1):317–23. [PubMed: 9398474]
7. Zhang Y, Li N, Yang Z. Perinatal food restriction impaired spatial learning and memory behavior and decreased the density of nitric oxide synthase neurons in the hippocampus of adult male rat offspring. Toxicology Letters. 2010; 193(2):167–72. [PubMed: 20079408]
8. Tonkiss J, Galler JR, Formica RN, Shukitt-Hale B, Timm RR. Fetal protein malnutrition impairs acquisition of a DRL task in adult rats. Physiol Behav. 1990; 48(1):73–7. [PubMed: 2122484]
9. Tonkiss J, Shultz PL, Shumsky JS, Fiacco TA, Vincitore M, Rosene DL, et al. Chlordiazepoxide-induced spatial learning deficits: dose-dependent differences following prenatal malnutrition. Pharmacol Biochem Behav. 2000; 65(1):105–16. [PubMed: 10638643]
10. Tonkiss J, Trzcinska M, Shultz PL, Vincitore M, Galler JR. Prenatally protein malnourished rats are less sensitive to the amnestic effects of medial septal infusions of chlordiazepoxide. Behav Pharmacol. 2000; 11(6):437–46. [PubMed: 11103910]
11. Austin-LaFrance RJ, Morgane PJ, Bronzino JD. Prenatal protein malnutrition and hippocampal functioning: rapid kindling. Brain Res Bull. 1991; 27(6):815–8. [PubMed: 1786559]
12. Bronzino JD, Austin-LaFrance RJ, Morgane PJ, Galler JR. Effects of prenatal protein malnutrition on kindling-induced alterations in dentate granule cell excitability. II. Paired-pulse measures. Exp Neurol. 1991; 112(2):216–23. [PubMed: 1903711]
13. Austin KB, Beiswanger C, Bronzino JD, Austin-LaFrance RJ, Galler JR, Morgane PJ. Prenatal protein malnutrition alters behavioral state modulation of inhibition and facilitation in the dentate gyrus. Brain Res Bull. 1992; 28(2):245–55. [PubMed: 1596745]
14. Bronzino JD, Blaise JH, Mokler DJ, Galler JR, Morgane PJ. Modulation of paired-pulse responses in the dentate gyrus: effects of prenatal protein malnutrition. Brain Res. 1999; 849(1–2):45–57. [PubMed: 10592286]
15. Luebke J, St John J, Galler JR. Prenatal protein malnutrition results in increased frequency of miniature inhibitory synaptic currents in rat CA1 pyramidal cells. Synapse. 2000; 37(1):23–31. [PubMed: 10842348]

16. Chang YM, Galler JR, Luebke JI. Prenatal protein malnutrition results in increased frequency of miniature inhibitory postsynaptic currents in rat CA3 interneurons. Nutr Neurosci. 2003; 6(4):263–7. [PubMed: 12887143]

17. Cintra L, Aguilar A, Granados L, Galvan A, Kemper T, DeBassio W, et al. Effects of prenatal protein malnutrition on hippocampal CA1 pyramidal cells in rats of four age groups. Hippocampus. 1997; 7(2):192–203. [PubMed: 9136049]

18. Cintra L, Diaz-Cintra S, Galvan A, Kemper T, Morgane PJ. Effects of protein undernutrition on the dentate gyrus in rats of three age groups. Brain Res. 1990; 532(1–2):271–7. [PubMed: 2282520]

19. Diaz-Cintra S, Cintra L, Galvan A, Aguilar A, Kemper T, Morgane PJ. Effects of prenatal protein deprivation on postnatal development of granule cells in the fascia dentata. J Comp Neurol. 1991; 310(3):356–64. [PubMed: 1787177]

20. Freund TF, Buzsaki G. Interneurons of the hippocampus. Hippocampus. 1996; 6(4):347–470. [PubMed: 8915675]

21. Klausberger T. GABAergic interneurons targeting dendrites of pyramidal cells in the CA1 area of the hippocampus. Eur J Neurosci. 2009; 30(6):947–57. [PubMed: 19735288]

22. Díaz-Cintra S, González-Maciel A, Morales MA, Aguilar A, Cintra L, Prado-Alcalá RA. Protein malnutrition differentially alters the number of glutamic acid decarboxylase-67 interneurons in dentate gyrus and CA1-3 subfields of the dorsal hippocampus. Exp Neurol. 2007; 208(1):47–53. [PubMed: 17706195]

23. Baude A, Bleasdale C, Dalezios Y, Somogyi P, Klausberger T. Immunoreactivity for the GABAA receptor alpha1 subunit, somatostatin and connexin36 distinguishes axoaxonic, basket, and bistratified interneurons of the rat hippocampus. Cereb Cortex. 2007; 17:2094–107. [PubMed: 17122364]

24. Lister JP, Blatt GJ, Debassio WA, Kemper TL, Tonkiss J, Galler JR, et al. Effect of prenatal protein malnutrition on numbers of neurons in the principal cell layers of the adult rat hippocampal formation. Hippocampus. 2005; 15(3):393–403. [PubMed: 15669101]

25. Rosene DL, Roy NJ, Davis BJ. A cryoprotection method that facilitates cutting frozen sections of whole monkey brains for histological and histochemical processing without freezing artifact. J Histochem Cytochem. 1986; 34(10):1301–15. [PubMed: 3745909]

26. West MJ, Slomianka L, Gundersen HJ. Unbiased stereological estimation of the total number of neurons in the subdivisions of the rat hippocampus using the optical fractionator. Anat Rec. 1991; 231(4):482–97. [PubMed: 1793176]

27. Katsumaru H, Kosaka T, Heizmann CW, Hama K. Immunocytochemical study of GABAergic neurons containing the calcium-binding protein parvalbumin in the rat hippocampus. Exp Brain Res. 1988; 72(2):347–62. [PubMed: 3066634]

28. Kosaka T, Katsumaru H, Hama K, Wu JY, Heizmann CW. GABAergic neurons containing the Ca2+-binding protein parvalbumin in the rat hippocampus and dentate gyrus. Brain Res. 1987; 419(1–2):119–30. [PubMed: 3315112]

29. Sloviter RS. Calcium-binding protein (calbindin-D28k) and parvalbumin immunocytochemistry: localization in the rat hippocampus with specific reference to the selective vulnerability of hippocampal neurons to seizure activity. J Comp Neurol. 1989; 280(2):183–96. [PubMed: 2925892]

30. Amaral DG, Witter MP. The three-dimensional organization of the hippocampal formation: a review of anatomical data. Neuroscience. 1989; 31(3):571–91. [PubMed: 2687721]

31. Rosene, DL.; Van Hoesen, GW. The hippocampal formation of the primate brain. A review of some comparative aspects of cytoarchitecture and connections. In: Jones, EG.; Peters, A., editors. Cerebral cortex. Vol. 7. New York: Plenum Publishing Corporation; 1987. p. 345-456.

32. Gundersen HJ, Jensen EB, Kieu K, Nielsen J. The efficiency of systematic sampling in stereology-reconsidered. J Microsc. 1999; 193(Pt 3):199–211. [PubMed: 10348656]

33. Gellerman LW. Chance orders of alternating stimuli in visual discrimination experiments. J Genet Psychol. 1933; 42:207–8.

34. Mouton, PR. Principles and practices of unbiased stereology: an introduction for bioscientists. Baltimore: Johns Hopkins University Press; 2002.

35. Hedreen JC. Lost caps in histological counting methods. Anat Rec. 1998; 250(3):366–72. [PubMed: 9517853]
36. Gundersen HJ. Stereology of arbitrary particles. A review of unbiased number and size estimators and the presentation of some new ones, in memory of William R, Thompson. J Microsc. 1986; 143(Pt 1):3–45. [PubMed: 3761363]
37. Sik A, Penttonen M, Ylinen A, Buzsaki G. Hippocampal CA1 interneurons: an in vivo intracellular labeling study. J Neurosci. 1995; 15(10):6651–65. [PubMed: 7472426]
38. Kosaka T. Axon initial segments of the granule cell in the rat dentate gyrus: synaptic contacts on bundles of axon initial segments. Brain Res. 1983; 274(1):129–34. [PubMed: 6616249]
39. Ramon y Cajal S. Estructura del asta de Ammon y fascia dentata. Ann Soc Esp Hist Nat. 1893; 22:53–114.
40. Soriano E, Frotscher M. A GABAergic axo-axonic cell in the fascia dentata controls the main excitatory hippocampal pathway. Brain Res. 1989; 503(1):170–4. [PubMed: 2611653]
41. Szentagothai J, Arbib MA. Conceptual models of neural organization. Neurosci Res Program Bull. 1974; 12(3):305–510. [PubMed: 4437759]
42. Li XG, Somogyi P, Tepper JM, Buzsaki G. Axonal and dendritic arborization of an intracellularly labeled chandelier cell in the CA1 region of rat hippocampus. Exp Brain Res. 1992; 90(3):519–25. [PubMed: 1385200]
43. Gilbert ME, Sui L, Walker MJ, Anderson W, Thomas S, Smoller SN, et al. Thyroid hormone insufficiency during brain development reduces parvalbumin immunoreactivity and inhibitory function in the hippocampus. Endocrinology. 2007; 148(1):92–102. [PubMed: 17008398]
44. Nomura T, Fukuda T, Aika Y, Heizmann CW, Emson PC, Kobayashi T, et al. Distribution of nonprincipal neurons in the rat hippocampus, with special reference to their dorsoventral difference. Brain Res. 1997; 751(1):64–80. [PubMed: 9098569]
45. Nomura T, Fukuda T, Aika Y, Heizmann CW, Emson PC, Kobayashi T, et al. Laminar distribution of non-principal neurons in the rat hippocampus, with special reference to their compositional difference among layers. Brain Res. 1997; 764(1–2):197–204. [PubMed: 9295210]
46. Buckmaster PS, Dudek FE. Neuron loss, granule cell axon reorganization, and functional changes in the dentate gyrus of epileptic kainate-treated rats. J Comp Neurol. 1997; 385(3):385–404. [PubMed: 9300766]
47. Dinocourt C, Petanjek Z, Freund TF, Ben-Ari Y, Esclapez M. Loss of interneurons innervating pyramidal cell dendrites and axon initial segments in the CA1 region of the hippocampus following pilocarpine-induced seizures. J Comp Neurol. 2003; 459(4):407–25. [PubMed: 12687707]
48. Diamond MC, Murphy GM, Akiyama K, Johnson RE. Morphologic hippocampal asymmetry in male and female rats. Exp Neurol. 1982; 76(3):553–65. [PubMed: 7084374]
49. Diamond MC, Johnson RE, Young D, Singh SS. Age-related morphologic differences in the rat cerebral cortex and hippocampus: male-female; right-left. Exp Neurol. 1983; 81(1):1–13. [PubMed: 6861939]
50. Ragbetli MC, Aydinlioglu A, Kaplan S. Sex differences and right-left asymmetries in rat hippocampal components. Int J Neurosci. 2002; 112(1):81–95. [PubMed: 12152407]
51. Toga AW, Thompson PM. Mapping brain asymmetry. Nat Rev Neurosci. 2003; 4(1):37–48. [PubMed: 12511860]
52. Tang, AC. A hippocampal theory of cerebral lateralization. In: Hugdahl, K.; Davidson, RJ., editors. The asymmetrical brain. Cambridge, MA: MIT Press; 2003. p. 37-68.
53. Xu Q, Cobos I, De La Cruz E, Rubenstein JL, Anderson SA. Origins of cortical interneuron subtypes. J Neurosci. 2004; 24(11):2612–22. [PubMed: 15028753]
54. Freund TF. Interneuron diversity series: rhythm and mood in perisomatic inhibition. Trends Neurosci. 2003; 26(9):489–95. [PubMed: 12948660]

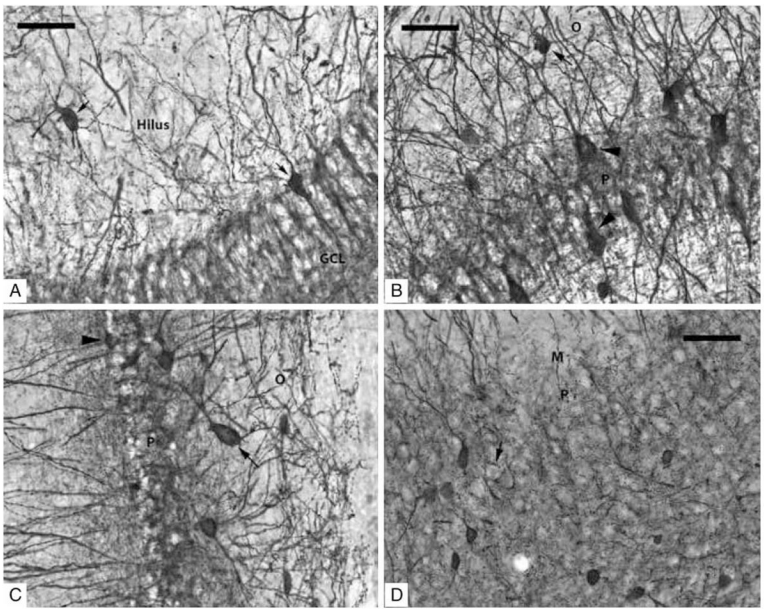

Figure 1.

(A–D) Photomicrographs taken with a 40× objective of PV-IR neurons in the subfields of the rat hippocampus. (A) Dentate Gyrus: short arrows indicate two PV-IR interneurons; one in the hilus and the other is inside the GCL. PV-IR fibers can be seen passing through both the hilus and the GCL where they are densely distributed in a 'honeycombed' fashion around granule cell somatas which are PV-IR negative. (B) CA3/2 subfield: several PV-IR interneurons are visible in both stratum pyramidale and oriens; an arrow indicates a darkly stained example in stratum oriens, and arrowheads indicate two examples of interneurons in the pyramidal layer. Unstained pyramidal neurons are responsible for the clear, 'honeycombed' appearance similar to the GCL. (C) CA1 subfield: a PV-IR interneuron located in the pyramidal layer is marked with an arrowhead; a PV-IR located just inside the stratum oriens is indicated by an arrow. (D) Subiculum: several PV-IR interneurons are clearly visible in the pyramidal layer. The location of an unstained pyramidal cell, surrounded by darkly stained contacts formed by the axons of PV-IR interneurons, is indicated by the arrow. Scale bars = 50 μm.

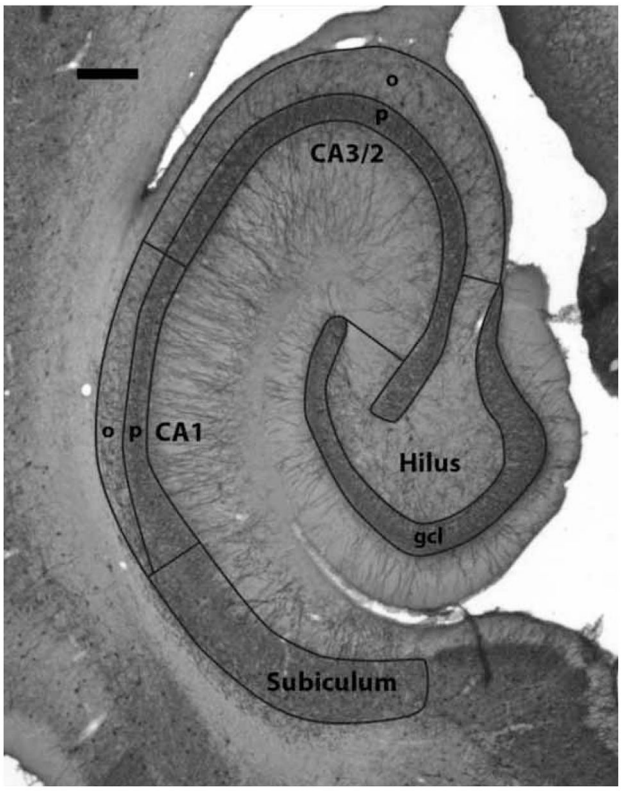

Figure 2.

Photomicrograph of a representative section of the hippocampal formation stained with an antibody for parvalbumin. The borders of the measured regions are outlined and labeled. Abbreviations in this and subsequent figures: gcl, granule cell layer; o, stratum oriens; p, stratum pyramidale. Scale bar = 500 μm.

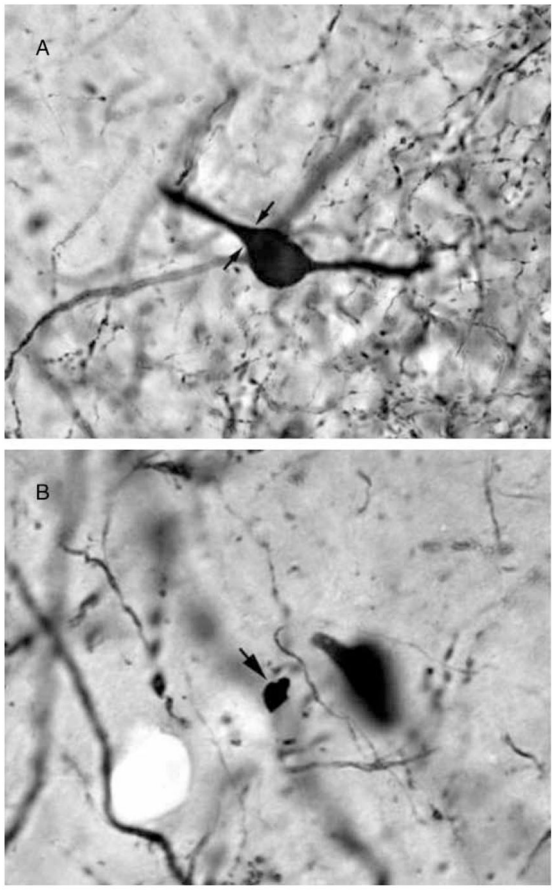

Figure 3.

These photomicrographs present examples of objects that would or would not be counted. (A) A stained neuron that qualified for counting due to the continuous border of the neuronal cell body and the stained processes extending from the soma. Arrows indicate the limit between the neuronal cell body and a stained process which, by itself, would not qualify as a countable object. (B) Arrow indicates a stained object that is not countable as a neuron. Note the lack of processes and the irregular border that is not consistent with neuronal morphology.

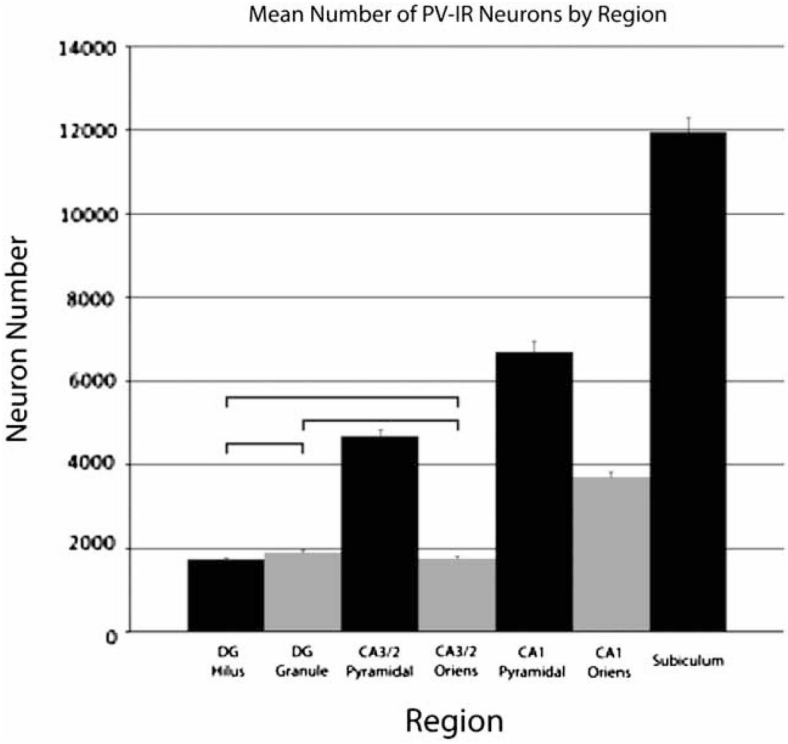

Figure 4.

Graph depicting the mean number of PV-IR neurons in the seven hippocampal subfields. Data are collapsed across the nutrition and hemisphere factors due to the lack of significant effects for those factors. A significant effect of the region factor was found; follow-up tests found significant differences in PV-IR neuron number in all comparisons except for the three indicated in the graph: the DG hilus, the DG granule cell layer, and the CA3/2 stratum oriens all had the same number of PV-IR neurons. Error bars are equal to the SEM.

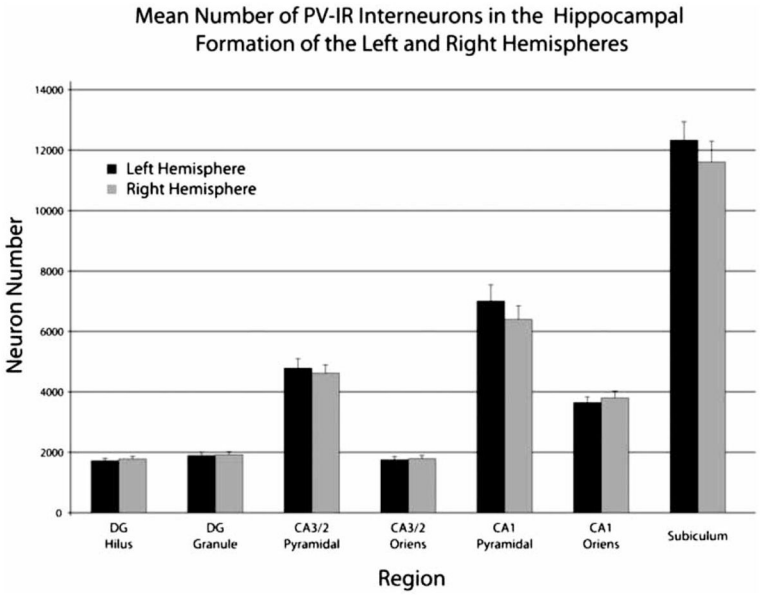

Figure 5.

Graph depicting the mean number of PV-IR interneurons estimated for left and right hippocampal formations by region and layer. Each bar represents the average number of PV-IR interneurons in the specified layer and includes data from both control and prenatally malnourished rats; error bars are equal to the SEM.

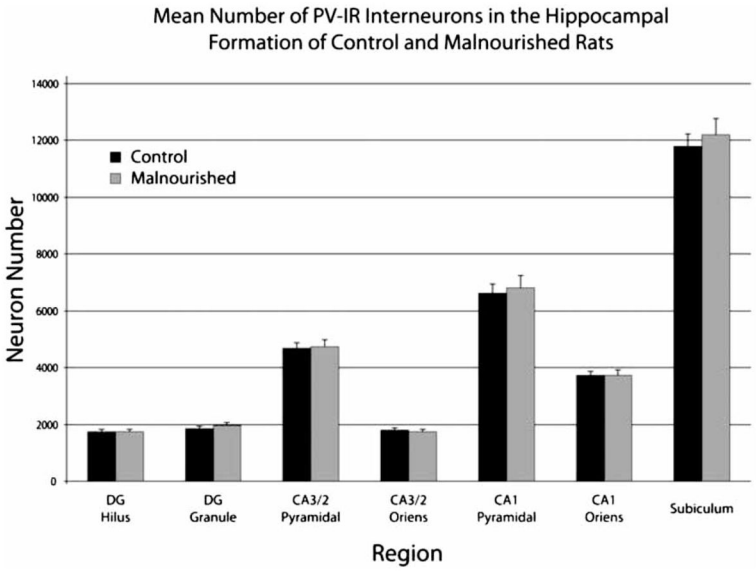

Figure 6.

Graph depicting the mean number of PV-IR interneurons estimated for control and prenatally malnourished rats by region and layer. Each bar represents the average number of PV-IR interneurons in the specified layer and includes data from both hemispheres; error bars are equal to the SEM.

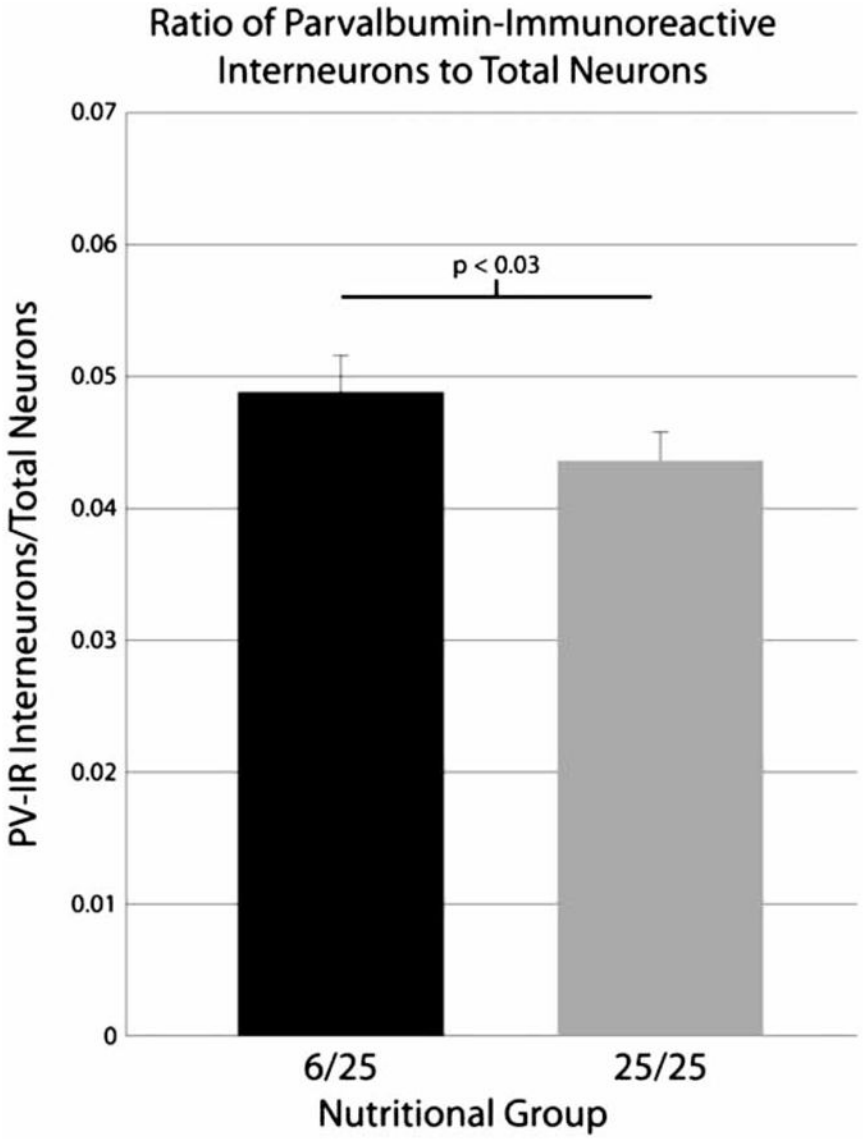

Figure 7.

Graph depicting the ratios of PV-IR interneurons to total neurons in the prenatally malnourished and control rats. There is a significant increase of 11.9% in this ratio for the prenatally malnourished animals. Data are collapsed across subfields due to the lack of a significant effect for the region factor; error bars are equal to the SEM. Total neuron data used in constructing ratios are taken from a prior study[1] as noted in the text.

Nutr Neurosci. Author manuscript; available in PMC 2014 August 20.

Table 1

Mean number of PV-IR interneurons

		DG hilus	DG granule	CA3/2 pyramidal	CA3/2 oriens	CA1 pyramidal	CA1 oriens	Subiculum
Left hemisphere								
6/25 Group	Mean	1701	1906	4636	1705	6879	3619	12 384
	CE	0.09	0.09	0.08	0.09	0.06	0.10	0.09
25/25 Group	Mean	1729	1884	4896	1786	7107	3663	12 288
	CE	0.09	0.09	0.08	0.09	0.06	0.10	0.09
Pooled 6/25 and 25/25	Mean	1716	1893	4782	1750	7007	3644	12 330
Right hemisphere								
6/25 Group	Mean	1804	2042	4827	1776	6757	3826	12 000
	CE	0.09	0.08	0.08	0.09	0.07	0.10	0.10
25/25 Group	Mean	1759	1824	4466	1806	6126	3790	11 307
	CE	0.09	0.09	0.08	0.09	0.07	0.10	0.10
Pooled 6/25 and 25/25	Mean	1779	1919	4624	1793	6402	3806	11 610

The mean number of PV-IR interneurons and coefficient of error (CE) for each group by hemisphere and region are listed.